Chemical Engineering Journal 498 (2024) 155296

Contents lists available at ScienceDirect

Chemical Engineering Journal

journal homepage: www.elsevier.com/locate/cej

Selective colorimetric sensors and diagnostic microfiber yarn for carbonyl groups via ion-pairing dyes with plural chromatic behaviors

Donghyun Kim, Jinho Lee, Seongcheol Ahn, Chungseong Park, Euichul Shin, Il-Doo Kim *

Department of Materials Science & Engineering, Korea Advanced Institute of Science and Technology (KAIST), 291 Daehak-ro, Yuseong-gu Daejeon 34141, Republic of Korea

ARTICLE INFO

Keywords:
Colorimetric sensor
Sensing array
Carbonyl group
Chromism
Diagnosis

ABSTRACT

An ideal chemo-responsive dye requires several essential features, including a facile preparation method, a broad range of dynamic color changes, and colorimetric responses to multiple stimuli. Herein, we present a simple and reliable procedure for synthesis of chemo-responsive dye from ion-pair formation of oppositely charged dyes. The ion-pairing dye exhibits various colorimetric responses to pH levels and amine concentrations, indicating that the dye has plural chromatic behaviors and wide visible spectrum: 'halochromism' and 'solvatochromism'. Due to this, our colorimetric sensors can selectively identify various carbonyl groups such as ketone, aldehyde, and carboxylic acid, in which the detection limits range from a minimum of 0.019 to maximum of 2.506 ppm. Furthermore, the sensing array composed of a single ion-pairing dye enables the generation of easily identifiable color-patterns as unique fingerprints for each carbonyl groups across a range of gas levels. Based on these colorimetric responses to carbonyl groups, we develop dye-loaded microfiber yarn for biomarker diagnosis, which can check for the presence of acetone gas in the exhaled breaths and confirm whether an individual is in the optimal ketosis state or not.

1. Introduction

Carbonyl group is a functional group consisting of a carbon atom double-bonded to an oxygen atom (C=O).[1] Carbonyl groups include some representative organic compounds such as ketone, aldehyde, and carboxylic acid, which have been used in various industries and researches. For example, acetone is the most widely used solvent in organic chemistry, and hazardous material to human health upon inhalation exposure to that (<100 ppm).[2,3] In addition, noninvasive diagnosis of diabetes can be achieved by exhaled breath analysis of acetone.[4–6] Formaldehyde is one of the most toxic air pollutants established by the World Health Organization (safe exposure standard: 0.08 ppm/30 min), causing cancer and gene mutation.[7,8] Acetic acid is an organic acid and widely used in various pharmaceutical and food industrial applications (50–60 g/L in vinegars).[9–12] Therefore, several spectroscopy and chromatography methods are typically employed to identify and differentiate these carbonyl groups, necessitating extensive space, prolonged processing time, and skilled personnel.[13–16] Consequently, there is a growing demand for sensing technologies with simplicity, reliability, and affordability.

Indeed, colorimetric sensors show potential for satisfaction of these demands.[17–20] Chemo-responsive dyes have been used as key materials in most of colorimetric sensors. Thus, the colorimetric sensors have been intensively developed on the basis of various intermolecular interactions of dyes with target analytes, such as dispersion force, hydrogen bonding, and dipole–dipole (or ion–dipole) interaction.[21–23] The interaction changes electrostatic potential (representing energies of π-delocalized electrons) of dyes, yielding colorimetric responses to the analytes.[24–26] Such chromatic behaviors are primarily classified as halochromism, solvatochromism, thermochromism, and others.[27–30] Based on these detection mechanisms, the synthesis and chemical modification of chemo-responsive dyes are considered an effective way to control the colorimetric responses of the sensors.[31–35] Nevertheless, this process often involves a high level of complexity and often unpredictable effect. Furthermore, the most synthetized and modified dyes generally exhibit a singular chromatic behavior, rendering them difficult to distinguish various analytes when using a single dye.[36,37].

To address this challenge, previous works have utilized a sensing array platform consisting of several dyes with different chromatic behaviors.[38,39] This platform mimics the biomimetic technology of the mammal olfactory system, employing cross-reactive sensory elements (i.

* Corresponding author.
E-mail address: idkim@kaist.ac.kr (I.-D. Kim).

https://doi.org/10.1016/j.cej.2024.155296
Received 12 June 2024; Received in revised form 13 August 2024; Accepted 28 August 2024
Available online 29 August 2024

e., chemo-responsive dyes) to generate composite color-patterns, serving as unique fingerprints for specific analytes. The presence of numerous dyes produces a sophisticated color-pattern, leading to better selectivity, reliability, and reproductivity. Unfortunately, it allows us to hinder and complicate an interpretation of the color-patterns. These complex arrays necessitate an image readout system equipped with additional devices to convert the color-patterns into identifiable signals. [40–42] Alternatively, the sensing arrays can be simplified by employing specific-responsive chemicals that react exclusively with target analytes, resembling an antigen–antibody reaction, thus eliminating the requirement for numerous chemo-responsive dyes.[43,44] However, these sensing arrays solely distinguish analogous analytes with same functional groups. For these reasons, developing a simple sensing array that is capable of distinguishing various targets becomes challenging.

Collectively, the necessity for a multitude of dyes in the sensing arrays arises from a singular chromatic behavior and the narrow visible spectrum of dyes. Thus, an ideal colorimetric sensor and sensing array with chemo-responsive dyes should have the following features. First, the synthesis of these dyes should be facile and should not involve any sophisticated procedures. Second, the chemo-responsive dyes should exhibit a broad range of colorimetric responses to various stimuli. Third, the color-patterns obtained from an ideal sensing array should be simple yet distinguishable for various analytes, without requiring additional devices.

Considering all the aforementioned demands, we present here a concise synthetic procedure for an ion-pairing dye that exhibits plural chromatic behaviors across a wide visible spectrum. Ion-pair formation is the process by which two ions with opposite charges, positive and negative, combine to form a single molecule through electrostatic attraction. Furthermore, this process can be easily achieved through simple mixing and precipitation. The ion-pairing dye responds to multiple stimuli such as pH and solvent variations (i.e., halochromism and solvatochromism), thereby enabling significantly greater range of coloration compared to previous chemo-responsive dyes. We prepared a colorimetric sensor and sensing array capable of identifying and distinguishing the carbonyl groups (e.g., acetone, acetic acid, and formaldehyde). In this sensing system, hydroxyl amine sulfate (HAS) and ethanol amine (EA) react to generate different products depending on carbonyl groups present. HAS reacts with acetone and formaldehyde to produce acetoxime and formaloxime, respectively. In contrast, EA reacts with acetic acid and formaldehyde to produce ethanol ammonium salt and N-methyl ethanol imine. These reactions generate distinct chemical environments based on the carbonyl groups, enabling visual identification through an ion-pairing dye with plural chromatic behaviors. Particularly, the concentration of EA is a key factor in controlling their sensitivity and selectivity. Owing to these unique properties, our sensing array consists of only a single dye (i.e., ion-pairing dye) with varying concentrations of EA, which generats highly simple and distinct color-patterns that serve as unique fingerprints for each carbonyl group across a range of gas levels. Using a customized electrospinning technique, we develop an ion-pairing dye-loaded microfiber yarn for biomarker diagnosis, specifically for detecting the presence of acetone gas in the exhaled breaths. This system allows for confirmation of whether the body burns fat for energy instead of glucose (i.e., ketosis state).

2. Experimental Section

2.1. Materials

Cresol red sodium salt was purchased from Tokyo Chemical Industry (Tokyo, Japan). Methanol (MeOH, 99.5 %), ethanol (EtOH, 99.5 %), and acetone (99.5 %) were obtained from Samchun Chemicals (Pyeongtaek, Republic of Korea). Other chemicals, including malachite green oxalate salt, HAS (99.999 %), EA (≥99.0 %), acetic acid (≥99.7 %), formaldehyde (37 wt% in H_2O), H_2O-d_2 (99.9 atom% D), dimethyl sulfoxide-d_6 (DMSO-d_6, 99.9 atom% D), and poly(vinyl alcohol) (PVA, Mw = 85,000–124,000 g mol^{-1}, >99 % hydrolyzed) were purchased from Sigma Aldrich (Missouri, United States) and used as-received. Deionized water was obtained from Clover Chemical (Chilgok, Republic of Korea).

2.2. Synthesis of ion-pairing dye

All synthetic procedures were conducted in air at room temperature (20–25 °C) and schematically illustrated in Fig. 1a. The materials were used without further purification. Initially, 0.01 M aqueous solutions of dyes were individually prepared by dissolving 1.16 g of malachite green oxalate salt and 1.11 g of cresol red sodium salt in 250 mL of deionized water, respectively. They were then mixed together for 12 h, resulting in a heterogeneous mixture due to the formation of water-insoluble solids (i.e., ion-pairing dye, MG–CR). This solid was precipitated by centrifugation (5000 rpm for 10 min) to remove unpaired dyes (i.e., MG and CR). Finally, the precipitate was dried under vacuum at room temperature for 24 h, yielding a 91 % product.

2.3. Preparation of colorimetric sensors and sensing array

The colorimetric sensor was prepared as follows: 4 mg of MG–CR and 500 mg of HAS were individually dissolved in 5 mL of MeOH and deionized water, respectively. The solutions were mixed for 10 min, followed by the addition of EA at various concentrations ranging from 0 to 12 vol%; the mixtures were stirred until uniform coloration was achieved. Finally, 30 μL of the mixtures were drop-cast onto a cellulose filter paper, and the solvent was evaporated at room temperature (20–25 °C). The sensing arrays were produced by similar procedures but with different chemical compositions, as listed in Table S1 (Supporting Information).

2.4. Chromatic analysis for carbonyl groups exposure

For saturated vapor-sensing measurements, 10 mL of the carbonyl groups (e.g., acetone, acetic acid, and formaldehyde) were dropped in a transparent crystallizing dish, sealed the dish with a glass plate. The sealed dish became filled with the saturated vapor of the carbonyl groups upon reaching equilibrium. The colorimetric sensors were then placed in the dish and illuminated using a white LED light. The photographic images were acquired and analyzed using a digital camera (Alpha 7 III, Sony, Tokyo, Japan) and graphic editing software (Adobe Photoshop, Adobe, California, United States). RGB values were extracted and averaged from each center of the element spots (31 by 31 pixels) to ensure colorimetric uniformity. Differential color maps were obtained by subtracting the RGB values before and after exposure to the carbonyl groups and then expanding the range to 0–255 for better visualization. Controlled gas-sensing measurements were conducted using a customized experimental setup, as shown in Fig. S1, Supporting Information. Mass flow controller (FC-280SAKZ, Celerity, California, United States) were employed to produce gas streams with desired levels of the carbonyl groups. The relative humidity (RH) was adjusted by mixing dry (0 % RH) and wet (100 % RH) air flow. The colorimetric sensors (or sensing arrays) were placed in a transparent gas chamber and exposed to controlled gas streams with a flow rate of 500 sccm. Images, RGB values, and differential color maps were obtained using the aforementioned methods.

2.5. Fabrication of dye-loaded microfiber yarn

First, 2 mg of MG–CR and 100 mg of HAS were individually dissolved in 5 mL of EtOH and deionized water, respectively. The solutions were mixed for 10 min, followed by the addition of EA (0.072 mL) and PVA (1 g). The mixture was stirred at 750 rpm and 70 °C for 12 h, yielding a clear yellow-green solution. This precursor solution was electrospun using two individual nozzles at a constant DC voltage applied between a

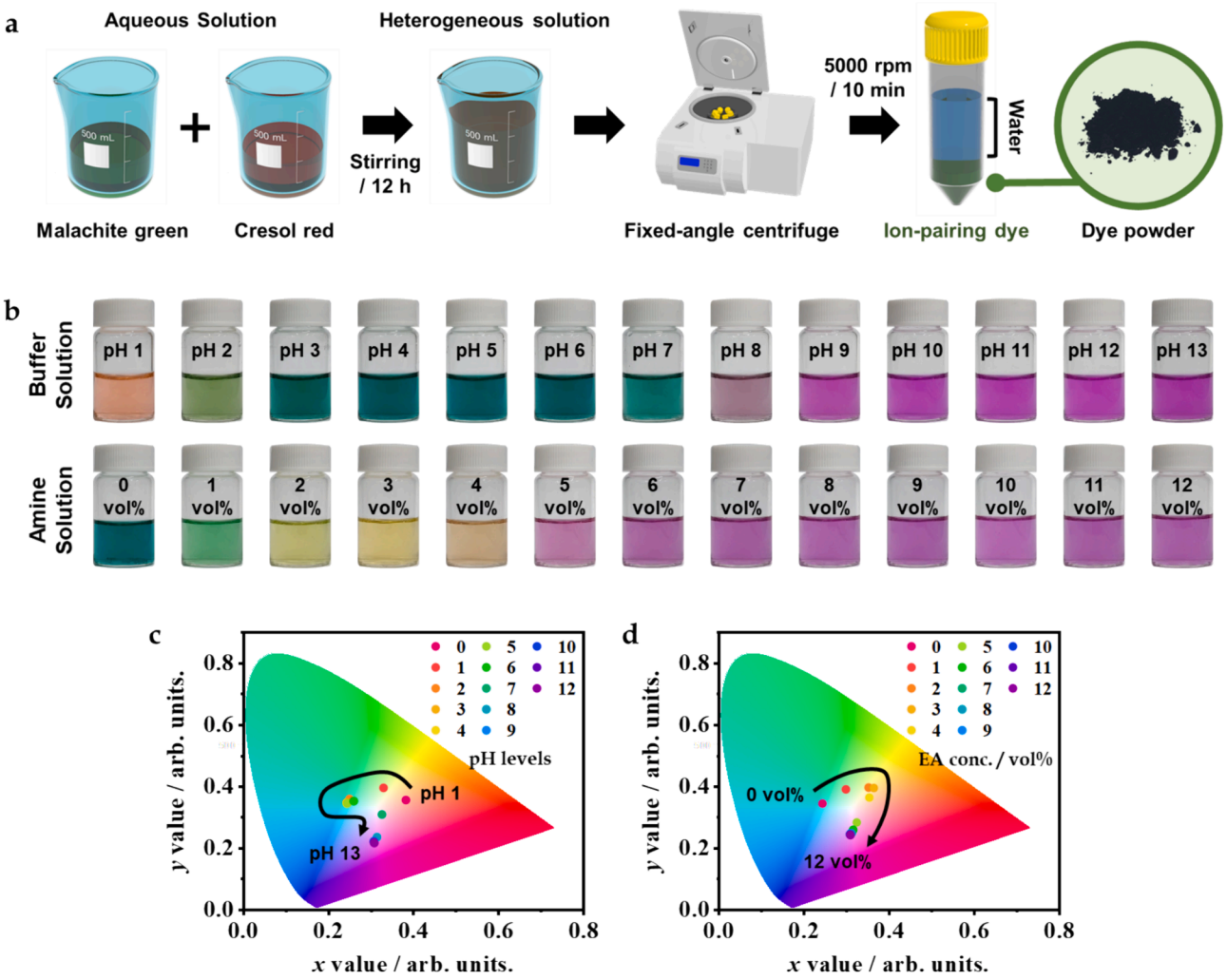

Fig. 1. Schematic illustration and chromatic behavior of ion-pairing dye. a Schematic of the synthetic procedure for ion-pairing dye through ion-pair formation between cationic and anionic dyes, MG and CR. b Color changes in the dye solutions across a range of pH levels (pH 1–13) and EA concentrations (0–12 vol%). c–d Corresponding CIE 1931 color spaces with chromaticity parameters denoted as *x* and *y* values, derived from their absorption spectra (Fig. S3, Supporting Information).

metal needle (19 gauge) and a rotary funnel collector, as listed in Table S2. During electrospinning, the humidity and temperature were maintained at approximately 45 % RH and 25 °C.

2.6. Characterization

^{1}H NMR analysis was conducted using an NMR spectrometer (AVANCE III 300, Bruker, Massachusetts, United States) at 300 MHz. The ^{1}H NMR sample of ion-pairing dye included a 0.01 wt% MG–CR solution in DMSO-d_6. Other samples were prepared as listed in Table S3, Supporting Information. The morphologies of the core wire and the microfiber yarn were observed using a scanning electron microscope (JSM-6360LV, JEOL, Tokyo, Japan) at an acceleration voltage of 5 kV. Absorbance spectra were acquired using a UV–Vis/NIR spectrophotometer (Lambda 1050, Perkin Elmer, Massachusetts, United States) in the wavelength range of 350–750 nm. Samples for halochromic analysis were prepared by adding 30 μL of a 0.1 wt% MG–CR solution in MeOH to 3 mL of the buffer solutions with various pH levels. Samples for solvatochromic analysis were prepared by adding 30 μL of a 0.1 wt% MG–CR solution to 3 mL of aqueous solutions with various EA concentrations.

3. Results and Discussion

3.1. Chromatic behaviors of ion-pairing dye

Our design strategy involves an ion-pair formation of oppositely charged dyes to obtain a chemo-responsive dye (i.e., ion-pairing dye) with plural chromatic behaviors and wide visible spectrum. Fig. 1a schematically presents a facile procedure for the synthesis of ion-pairing dye (MG–CR). Malachite green (MG) and cresol red (CR) were selected as cationic and anionic dyes, respectively, based on their charges, colorations, and ionic interactions. We mixed two aqueous solutions of the dyes and immediately obtained heterogeneous mixture with water-insoluble solid. The formation of this solid is attributed to an increase in hydrophobicity of an ion-pairing dye.[45,46] The resultant change in water solubility facilitates the precipitation of the ion-pairing dye (i.e., water-insoluble solid) in aqueous media. This also allows to the complete purification of the dye (MG–CR) without further processes, as confirmed by ^{1}H NMR spectroscopy (Fig. S2, Supporting Information). ^{1}H NMR spectrum of MG–CR revealed that oppositely charged dyes were combined in a certain molar ratio to achieve charge neutrality, especially MG:CR=1:1. To demonstrate chromatic behavior of MG–CR, we prepared and photographed the aqueous solutions containing MG–CR at various pH levels and EA concentrations (Fig. 1b). We observed a

variation in coloration across the pH range from 1 to 13; the dye solutions changed from orange to green in the pH range of 1–3 and to violet at pH>8. The color change was also observable across the entire range of EA concentrations; their coloration changed from green to yellow to violet with increasing EA concentrations. To clarify these changes, we acquired the absorption spectra of the dye solutions and then converted them into the *x* and *y* values defined by the International Commission of Illumination (CIE) 1931 color space (Fig. S3, Table S4, Supporting Information).[47] The dye solutions showed entirely different *x* and *y* values with changes in pH levels and EA concentrations. As listed in Table S4, the *x* value increased up to 3 vol% of EA, and then decreased with higher EA concentrations. However, no clear pattern was observed for pH levels. On the other hand, the highest *y* values were observed at pH 2 and 2 vol% EA, followed by a gradual decrease in *y* values with increasing pH levels and EA concentrations. These shifts in *x* and *y* values yielded the S-shaped and reverse C-shaped curves spanning a broad CIE color space, respectively (Fig. 1c and 1d). Therefore, MG–CR clearly shows distinctive colorimetric responses to not only pH levels but

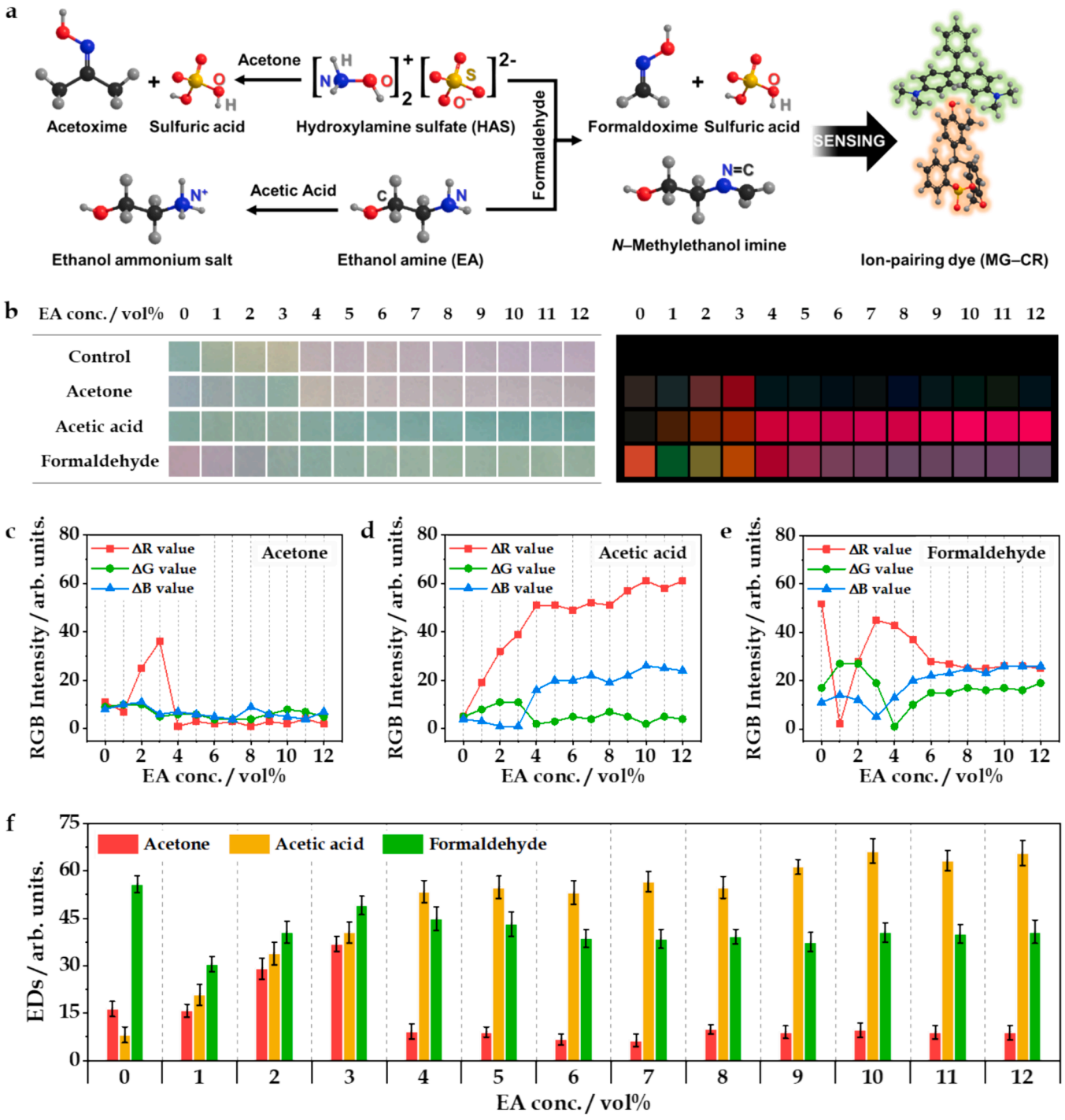

Fig. 2. Detection of carbonyl groups by colorimetric sensors with ion-pairing dye. a Suggested mechanism of chemical and optical changes in the colorimetric sensor in response to different carbonyl groups. b Color changes (left) and differential color maps (right; RGB range of 0–62 expanded to 0–255) of the sensors with a series of EA concentrations upon exposure to saturated vapors after 20 min. c–e Corresponding RGB differential profiles for acetone, acetic acid, and formaldehyde, respectively. f Response plots of EDs resulting from the color changes in the sensors as a function of EA concentration.

also amine concentrations, indicating that MG–CR has plural chromatic behaviors, "halochromism" and "solvatochromism." Compared to previous chemo-responsive dyes, the synthesis procedure for MG–CR is notably simple, requiring no specific condition control, such as pH, temperature, and catalyst. Additionally, MG–CR exhibits a range of colorations, including pink, light green, deep green, violet, and yellow. [48–50].

3.2. Mechanism for colorimetric responses to carbonyl groups

Based on these chromisms, we fabricated a colorimetric sensor using MG–CR to identify carbonyl groups such as ketone, carboxylic acid, and aldehyde. Then, we selected acetone, acetic acid, and formaldehyde as representatives of the carbonyl groups, respectively. To distinguish these carbonyl groups, HAS and EA were incorporated within the colorimetric sensors. As shown in Fig. 2a, HAS reacts with acetone and formaldehyde, producing acetoxime and formaloxime, respectively. However, acetic acid does not react with HAS.[51,52] Similarly, EA exhibits selective reactions with acetone, acetic acid, and formaldehyde. [53] These reactions can generate different products depending on such carbonyl groups, leading to various chemical environments of colorimetric sensors. The plural chromatic behaviors of MG–CR enabled visual identification of these variations. As a result, our sensors showed distinct colorimetric responses (left) and differential color maps (right) upon exposure to carbonyl groups, as shown in Fig. 2b (for the full color changes, see Fig. S4–S6, Supporting Information). Moreover, their RGB differential profiles and Euclidean distances (EDs, defined as the square root of the sum of different RGB values) plots provided a quantification of these color changes and enabled complete discrimination of the carbonyl groups (Fig. 2c–f and Table S5).[54,55] For acetone, color changes were observed within an EA concentration range of 0–3 vol%. However, Variation in chemical environments caused by HAS-acetone reaction is negligible at higher EA concentrations, resulting from the limited amount of HAS in the sensors. Thus, no color changes were observed at concentrations above 4 vol% of EA, regardless of exposure to acetone. On the other hand, as EA reacts with both carboxylic acid and aldehyde, the sensors exhibited significant color changes upon exposure to acetic acid and formaldehyde even at entire EA concentrations. The

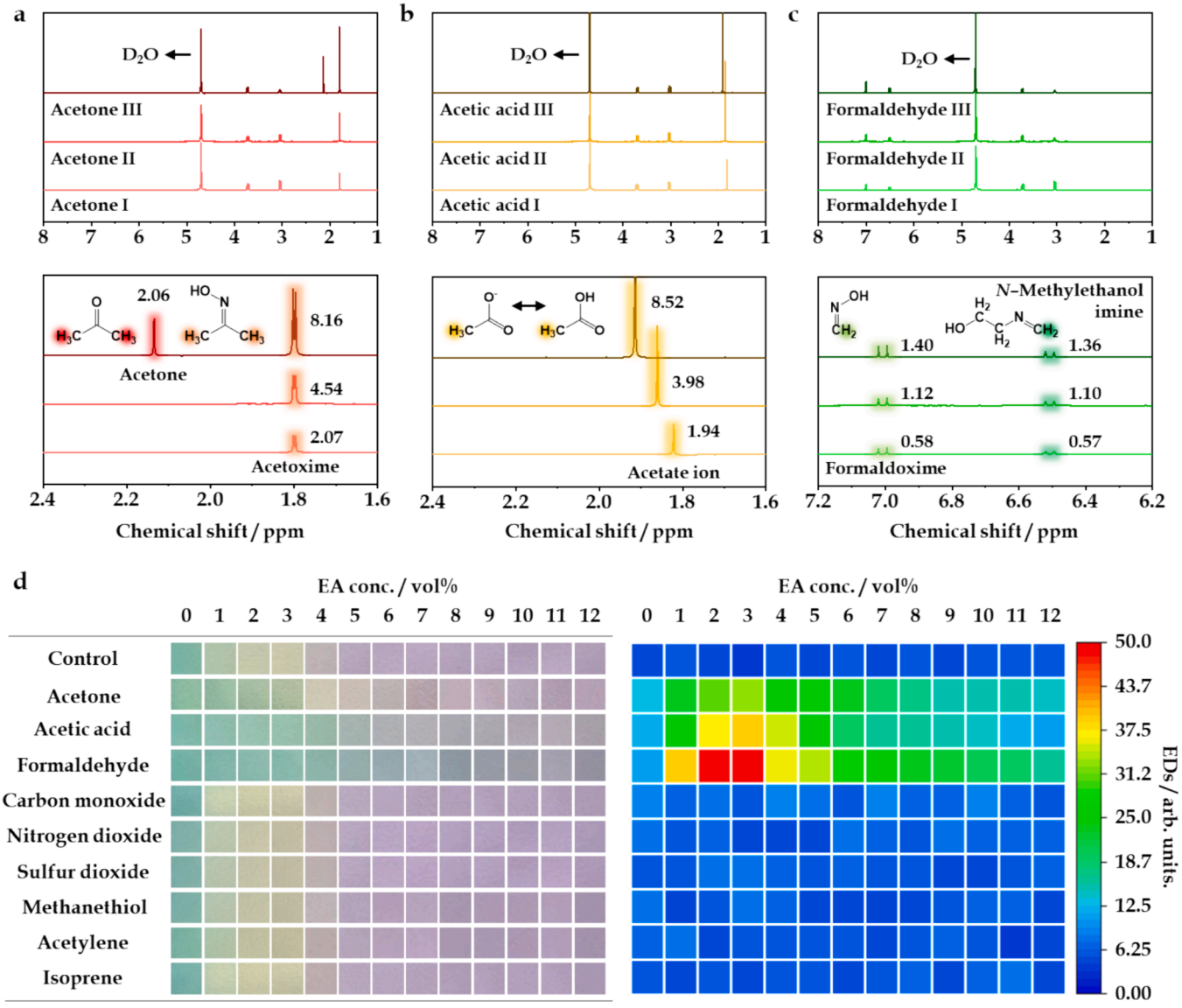

Fig. 3. Spectroscopic and selectivity analyses of colorimetric sensors based on suggested mechanism. a–c ^{1}H NMR spectra (top row) and their enlarged spectra (bottom row) of HAS+EA solution (in deuterium oxide, H_2O-d_2) with various amounts of acetone, acetic acid, and formaldehyde, respectively (inset numbers within spectra = peak areas). d Color changes (left) of our sensors upon exposure to a series of gases at 20 ppm and corresponding 2D contour plots (right) by color mapping to EDs on a 2D format.

color changes were visually similar within an EA concentration range of 3–12 vol% for acetic acid and formaldehyde, but their RGB values and EDs were significantly different from each other. In addition, their color change rates varied significantly depending on EA concentrations, as shown in Fig. S5 and S6 (Supporting Information); higher EA concentrations resulted in lower rates of color change. On the basis of suggested mechanism, these results demonstrate that our sensors uniquely interact with individual carbonyl groups, and EA concentration is a major factor affecting the colorimetric response of our sensors. Therefore, the visual distinctions of carbonyl groups can be achieved using the ion-pairing dye (i.e., MG–CR) that exhibits plural chromatic behaviors.

3.3. Selectivity and sensitivity of colorimetric sensors

The spectroscopic analysis was also in a good agreement with our mechanism, indicating that HAS and EA differently react with carbonyl groups and then generate different products. Fig. 3a–c shows the ^{1}H NMR spectra of a mixed aqueous solution containing HAS and EA with various amounts of acetone, acetic acid, and formaldehyde; their amounts gradually increased in the order of I, II, and III, as listed in Table S3. As shown in Fig. 3a, methyl groups (–CH_3) in acetoxime appeared at 1.80 ppm and this peak area was proportional to acetone amount. Then, we observed a single chemical shift of acetone's methyl groups at 2.13 ppm only in Acetone III, resulting from acetone remaining after reacting with HAS. On the other hand, as depicted in Fig. 3b, the peak transitioned from 1.82 to 1.91 ppm with increasing amount of acetic acid. This result clearly indicates the gradual increase of acetate ions (i.e., conjugate base of acetic acid) produced from acid-base reaction of acetic acid and EA.[56] Fig. 3c shows two individual peaks of 6.51 and 7.01 ppm for imine groups (–N=CH_2) in formaldoxime and *N*-methylethanol imine, consistent with suggested mechanism in Fig. 2a. These chemical reactions were specific to carbonyl groups such as ketone, carboxylic acid, and aldehyde. As a result, our sensors exhibit a selective response to acetone, acetic acid, and formaldehyde. Fig. 3d displays color changes (left) and 2D contour plots (right) of the sensors upon exposure to a series of gases. Indeed, color changes were observed specifically for the carbonyl groups, but not for other functional groups, indicating the sensors' selectivity towards detecting carbonyl-containing compounds. In addition, the EDs for carbonyl groups were larger than those for other functional groups, facilitating the identification of whether the target analyte is a carbonyl group or not, as confirmed by their 2D contour plots (Table S6–S8, Supporting Information). Moreover, we could adjust the sensors' sensitivity to these carbonyl groups in the same mechanism. When exposed to carbonyl groups at levels ranging from 0.5 to 20 ppm, our sensors showed distinct color changes depending on both the gas levels and EA concentrations (Fig. S7, Supporting Information). Therefore, the sensors exhibited different EDs at different gas levels, enabling quantitative estimation of the limit of detection (LOD). The LOD was defined as three times the standard deviation plus the mean of the blank control, as shown in Fig. S8–S10 (Supporting Information). The sensitivity increased with increasing EA concentration up to 3 vol%, but gradually decreased above 4 vol% (Table 1). These trends were consistent across all carbonyl groups such as acetone, acetic acid, and formaldehyde. The LOD, especially for acetic acid, could fluctuate by as much as ~60 orders of magnitude. As a result, the colorimetric sensors based on suggested mechanism are successful in controlling not only selectivity but also sensitivity to the carbonyl groups.

3.4. Sensing array for discrimination between carbonyl groups

Due to these variations in colorimetric responses to gases, we were able to develop a sensing array composed of only three sensory elements, capable of discriminating between carbonyl groups and their gas levels. As shown in Fig. 4a, our sensing array displayed the composite color-patterns at a series of gas levels (from 0.5 to 20 ppm), creating a unique fingerprint for individual carbonyl group. For example, the first element of the sensing array exhibited a green color after exposure to all carbonyl groups, indicating their presence in the surroundings. The coloration of the second element changed from violet to yellow for acetone, but to green for acetic acid and formaldehyde, thereby distinguishing acetone from the other carbonyl groups. To differentiate between acetic acid and formaldehyde, we employed the third element with higher EA concentration than other elements. This element exhibited color changes upon exposure to acetic acid, which were distinct from those observed for formaldehyde, allowing for their differentiation. The EDs of our sensing array were also significantly different depending on the gas levels of acetone, acetic acid, and formaldehyde, enabling discrimination of their gas levels (Fig. 4b–d). Based on their RGB values, we conducted a principal component analysis (PCA), representing a linear combination of the dataset obtained from five independent trials (Fig. 4e).[57] The PCA result necessitates at least five dimensions to capture more than 95 % of the total variance for an accurate classification (Fig. 4f). However, for simplicity and clarity, we only used the first two principal components (PC1 and PC2), which captured almost 80 % of the total variance, in creating the PCA score plot. As shown in Fig. 4e, all individual datasets were classified into distinct clusters for each carbonyl group and even showed a discernible tendency on a series of gas levels with good resolution. These results indicate that our sensing array, consisting of a single dye (MG–CR) with different EA concentrations, facilitates the identification of carbonyl groups through a highly simple color-pattern, serving as a unique fingerprint for each carbonyl group across a range of gas levels. Importantly, this identification could be achieved without the need for numerous dyes and additional devices.

3.5. Dye-loaded microfiber yarn for biomarker diagnosis

Furthermore, considering the carbonyl groups as biomarkers, we utilized our sensors for the potential diagnosis of a variety of diseases based on exhaled breath gas analysis. To demonstrate a feasibility of colorimetric sensors for the biomarker diagnosis, we fabricated a dye-loaded microfiber yarn through a customized electrospinning technique (Fig. 5a and b). The polymer for fabrication of dye-loaded microfiber yarn should possess the following features. First, the polymer should be completely dissolved in both water and alcohol. Second, precursor solution of polymer should be electrospun at lower voltage and shorter distance than in conventional electrospinning. Third, the polymeric fibers should have appropriate tension to maintain a yarn structure during our customized electrospinning process. For these

Table 1
Estimation of LOD for carbonyl groups with various EA concentrations.

EA conc. / vol%		0	1	2	3	4	5	6
LOD / ppm	Acetone	1.178	0.099	0.024	0.019	0.022	0.061	0.069
	Acetic acid	0.200	0.065	0.059	0.042	0.062	0.080	0.245
	Formaldehyde	0.346	0.137	0.109	0.083	0.086	0.093	0.136
EA conc. / vol%		7	8	9	10	11	12	
LOD / ppm	Acetone	0.093	0.123	0.132	0.156	0.218	0.228	
	Acetic acid	0.290	0.407	0.875	1.054	1.884	2.506	
	Formaldehyde	0.221	0.450	0.516	0.616	0.766	1.250	

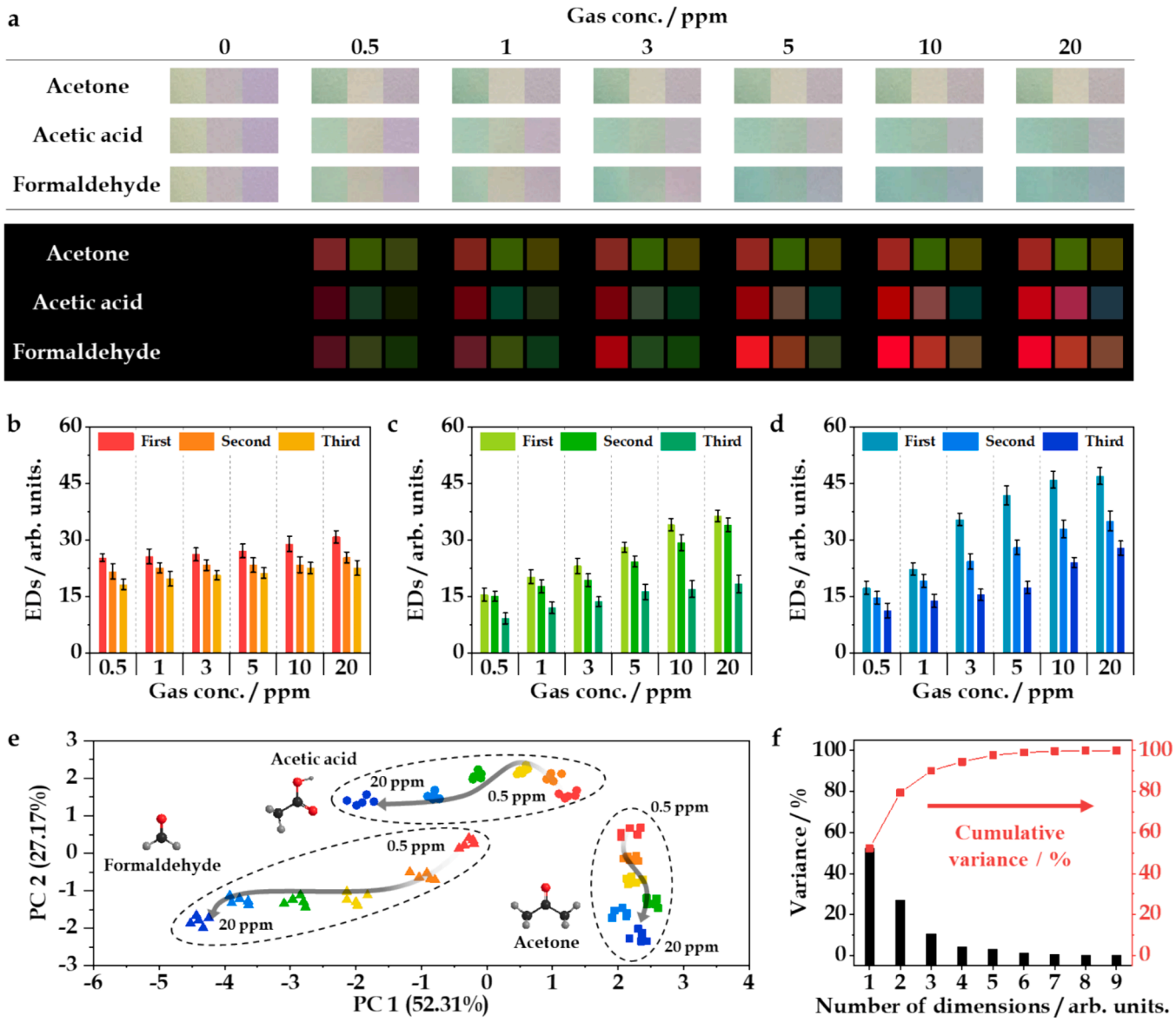

Fig. 4. Discrimination between carbonyl groups of various levels by sensing array consisting of ion-pairing dye. a Color-patterns (top row) and differential color maps (bottom row; RGB range of 0–46 expanded to 0–255) of the sensing array upon exposure to carbonyl groups at a series of gas levels for 1 h (for details, Table S1, Supporting Information). b–d Response plots of EDs resulting from the color changes in three sensory elements of the sensing array as a function of gas levels for acetone, acetic acid, and formaldehyde, respectively. e PCA score plots using the first two principal components for carbonyl groups and their gas levels in five independent trials. f Cumulative PCA screen plot from the RGB values of all three sensory elements.

reasons, we chose PVA as the polymer to produce microfiber yarn through the electrospinning. The two feeding solutions were electrospun onto the rotary funnel collector, which in turn the electrospun microfibers were wound on the commercial core wire. The microfibers were continuously produced from the solutions and then removed by the core wire, resulting in the formation of a core-support wire/shell-microfiber bundle of yarn structure. In this procedure, we observed a stable microfiber cone when the production and removal rates of microfibers are exactly equal (Fig. 5b). As shown in Fig. 5d–g, the scanning electron microscopy (SEM) images show that the core wire consists of microfibers with average diameters of approximately 9.82 and 15.3 μm. However, the prepared yarn was uniformly covered with thinner microfibers (1.29 μm of diameter), which allow gas molecules to easily permeate the porous matrix, leading to good sensitivity and short response time to target analytes.[58,59] A simulated breath test with a biomarker was systematically performed by the experimental setup, in which we collected real exhaled breaths from 15 individual healthy subjects labeled with the letters “A” to “O” (Fig. 5c). The breath samples were extracted from Tedlar bags using a diaphragm pump and subsequently mixed with 10 ppm of acetone gas to generate a gas mixture that simulates the exhaled breath of a human in a ketosis state, where fat is used for energy instead of glucose.[60,61] When exposed to the simulated breaths, the microfiber yarn exhibited distinct color change from light-yellow to green (Fig. 5h). Furthermore, we compared the colorimetric responses to two different breath samples; one containing acetone gas, and the other without acetone gas. As shown in Fig. 5i, although there is a slight variation in EDs depending on the subjects, we clearly observed the differences between EDs upon exposure to the two different breath samples. Specifically, the EDs ranged from 68.75 to 87.5 when exposed to the breath samples with acetone gas. In contrast, upon exposure to the breath samples without acetone gas, the EDs fell within a much lower range (from 0 to 10). Similarly, their corresponding RGB color spaces show a distinct grouping with sufficient separability between the two different breath samples (Fig. 5j). Therefore, this system can detect the

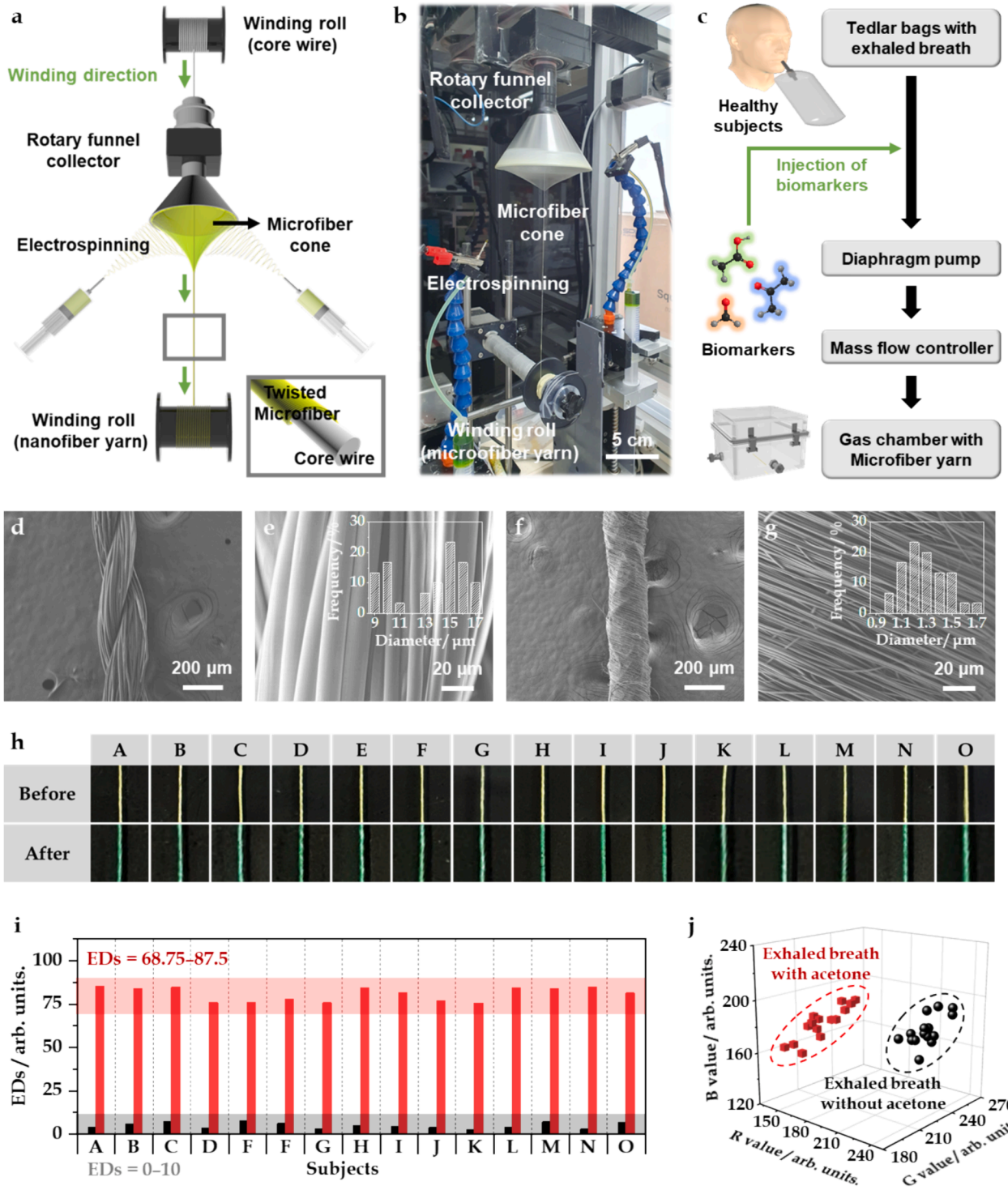

Fig. 5. Development of dye-loaded microfiber yarn for biomarker diagnosis. a and b Schematic and photograph of the fabrication of microfiber yarn using customized electrospinning technique. c Experimental setup for the biomarker analysis in exhaled breath samples. d–g SEM images of the core wire and the prepared microfiber yarn, respectively (inset: fiber diameter distribution). h Color changes in the yarn before and after exposure to the simulated breath samples with acetone gas as biomarker for 10 min (subjects: A to O). i Response plots of EDs resulting from the color changes in the yarns as a function of subjects. j Corresponding RGB color space showing the two clusters separated by the presence and absence of acetone gas in the exhaled breath samples.

presence of acetone gas in the exhaled breaths and confirm whether an individual is in the optimal ketosis state or not. This result visually communicates important information for diagnosing biomarkers (e.g., ketosis) and monitoring healthy metabolism.

4. Conclusions

In this study, we demonstrated that the ion-pair formation of oppositely charged dyes is an effective method to obtain a chemo-responsive dye, specifically ion-pairing dye, exhibiting multiple chromatic behaviors and a wide visible spectrum. Compared to previous work, our ion-

pairing dye (MG–CR) was obtained from highly simple synthetic procedure without controlling any condition. The dye also showed diverse color changes with varying pH levels and EA concentrations, indicating that MG–CR intrinsically has two chromatic behaviors, including both "halochromism" and "solvatochromism." Based on these chromisms, we prepared colorimetric sensors composed of HAS and EA to identify carbonyl groups such as acetone, acetic acid, and formaldehyde. On the basis of our suggested mechanism, HAS and EA differently react with the carbonyl groups, generating different chemical environments. These variations could be visually identified by MG–CR owing to its halochromism and solvatochromism. In addition, the colorimetric responses to the carbonyl groups are easily adjusted by EA concentrations, in which theoretical detection limit, especially for acetic acid, could fluctuate by as much as ~60 orders of magnitude. Due to these unique features, our sensing array, consisting of only a single dye with varying EA concentrations, successfully differentiated between the carbonyl groups across a range of gas levels from 0.5 to 20 ppm. The composite color-patterns from the sensing array were highly simple and visually identifiable, eliminating the need for numerous dyes and additional devices. Moreover, we employed a customized electrospinning technique to develop dye-loaded microfiber yarn for biomarker diagnosis. The microfiber yarn can detect the presence of acetone gas in the exhaled breaths and confirm whether an individual is burning fat for energy instead of glucose (i.e., ketosis state). Consequently, we propose a robust strategy to overcome the challenges commonly encountered with typical colorimetric sensors and expect that our findings will serve as an advanced technology for colorimetric sensor systems.

CRediT authorship contribution statement

Donghyun Kim: Writing – original draft, Visualization, Methodology, Investigation, Formal analysis, Data curation, Conceptualization. **Jinho Lee:** Software, Resources, Formal analysis, Data curation. **Seongcheol Ahn:** Writing – original draft, Validation, Software, Resources, Data curation. **Chungseong Park:** Visualization, Methodology, Investigation, Conceptualization. **Euichul Shin:** Software, Resources, Methodology, Investigation, Conceptualization. **Il-Doo Kim:** Writing – review & editing, Validation, Supervision, Project administration, Funding acquisition.

Declaration of competing interest

The authors declare that they have no known competing financial interests or personal relationships that could have appeared to influence the work reported in this paper.

Data availability

Data will be made available on request.

Acknowledgement

This work was supported by the National Research Foundation of Korea (NRF) grant funded by the Korea government, Ministry of Science and ICT (Development of Nanofiber Yarn Based Compound Sensor as a Comprehensive Wearable Healthcare Solution) (Grant No. RS-2024-00357296)

Appendix A. Supplementary material

Supplementary material to this article can be found online at https://doi.org/10.1016/j.cej.2024.155296.

References

[1] J. Otera, Modern carbonyl chemistry, Wiley-VCH, Weinheim, 2000.
[2] R. Remler, The solvent properties of acetone, Ind. Eng. Chem. 15 (1923) 717–720, https://doi.org/10.1021/ie50163a023.
[3] W.E. Luttrell, A.L. LaGrow, Acetone, J. Chem. Health Saf. 21 (2014) 29–31, https://doi.org/10.1016/j.jchas.2014.03.006.
[4] N. Teshima, J. Li, K. Toda, P.K. Dasgupta, Determination of Acetone in Breath, Anal. Chim. Acta 535 (2005) 189–199, https://doi.org/10.1016/j.aca.2004.12.018.
[5] M.Y. Chuang, Y.T. Lin, T.W. Tung, L.Y. Chang, H.W. Zan, H.F. Meng, C.J. Lu, Y. T. Tao, Room-temperature-operated Organic-based Acetone Gas Sensor for Breath Analysis, Sens. Actuat. B 260 (2018) 593–600, https://doi.org/10.1016/j.snb.2017.12.168.
[6] I.C. Weber, H.P. Braun, F. Krumeich, A.T. Güntner, S.E. Pratsinis, Superior acetone selectivity in gas mixtures by catalyst-filtered chemoresistive sensors, Adv. Sci. 7 (2020) 2001503, https://doi.org/10.1002/advs.202001503.
[7] World Health Organization, Air Quality Guidelines for Europe, WHO Regional Office for Europe, Copenhagen, 2000.
[8] T. Salthammer, S. Mentese, R. Marutzky, Formaldehyde in the indoor environment, Chem. Rev. 110 (2010) 2536–2572, https://doi.org/10.1021/cr800399g.
[9] W.E. Luttrell, Acetic Acid, J. Chem. Health Saf. 19 (2012) 37–38, https://doi.org/10.1016/j.jchas.2012.09.008.
[10] L. Solieri, P. Giudici, Vinegars of the World, In Vinegars of the World, Springer Milan, Milano, 2009.
[11] S. Lucas, The pharmacology of indomethacin, Headache 56 (2016) 436–446, https://doi.org/10.1111/head.12769.
[12] T. Kobayashi, Y. Ohta, J. Yoshino, S. Nakazawa, Teprenone promotes the healing of acetic acid-induced chronic gastric ulcers in rats by inhibiting neutrophil infiltration and lipid peroxidation in ulcerated gastric tissues, Pharmacol. Res. 43 (2001) 23–30, https://doi.org/10.1006/phrs.2000.0748.
[13] J.P. McEvoy, Characterizing carbonyls with infrared spectroscopy: an introductory chemistry experiment in a molecular bioscience program, J. Chem. Educ. 91 (2014) 726–729, https://doi.org/10.1021/ed4001427.
[14] C. Lievens, D. Mourant, M. He, R. Gunawan, X. Li, C.Z. Li, An FT-IR spectroscopic study of carbonyl functionalities in bio-oils, Fuel 90 (2011) 3417–3423, https://doi.org/10.1016/j.fuel.2011.06.001.
[15] H. Zhu, X. Li, C.F. Shoemaker, S.C. Wang, Ultrahigh performance liquid chromatography analysis of volatile carbonyl compounds in virgin olive oils, J. Agric. Food Chem. 61 (2013) 12253–12259, https://doi.org/10.1021/jf404368m.
[16] F.D. Gonçalves, M.L. Almeida, J.M. Martins, L.H. Carvalho, J.A. Rodrigues, R. M. Ramos, Gas-diffusion microextraction combined with HPLC-DAD for the comprehensive analysis of volatile carbonyl compounds in wood-based panels, Talanta 272 (2024) 125818, https://doi.org/10.1016/j.talanta.2024.125818.
[17] D. Kim, K.S. Hwang, J.H. Kim, C. Lee, J.Y. Lee, Multituning of structural color by protonation and conjugate bases, ACS Appl. Polym. Mater. 3 (2021) 2902–2910, https://doi.org/10.1021/acsapm.0c01382.
[18] D. Kim, K.S. Hwang, W.G. Koh, C. Lee, J.Y. Lee, Volatile organic compound sensing array and optoelectronic filter system using ion-pairing dyes with a wide visible spectrum, Adv. Mater. 34 (2022) 2203671, https://doi.org/10.1002/adma.202203671.
[19] J. Yoon, S.K. Chae, J.M. Kim, Colorimetric Sensors for Volatile Organic Compounds (VOCs) based on conjugated polymer-embedded electrospun fibers, J. Am. Chem. Soc. 129 (2007) 3038–3039, https://doi.org/10.1021/ja067856+.
[20] Y. Duan, H. Lin, P. He, Q. Chen, Detection of volatile marker in the wheat infected with aspergillus flavus by porous silica nanospheres doped bodipy dyes, Sens. Actuat. B 330 (2021) 129407, https://doi.org/10.1016/j.snb.2020.129407.
[21] X. Wang, X. Sun, P.A. Hu, J. Zhang, L. Wang, W. Feng, S. Lei, B. Yang, W. Cao, Colorimetric sensor based on self-assembled polydiacetylene/graphene-stacked composite film for vapor-phase volatile organic compounds, Adv. Funct. Mater. 23 (2013) 6044–6050, https://doi.org/10.1002/adfm.201301044.
[22] J.H. Fu, Z. Zhong, D. Xie, Y.J. Guo, D.X. Kong, Z.X. Zhao, Z.X. Zhao, M. Li, SERS-active MIL-100 (Fe) sensory array for ultrasensitive and multiplex detection of VOCs, Angew. Chem. 132 (2020) 20670–20679, https://doi.org/10.1002/ange.202002720.
[23] M.M. Bordbar, J. Tashkhourian, B. Hemmateenejad, Structural elucidation and ultrasensitive analyses of volatile organic compounds by paper-based nano-optoelectronic noses, ACS Sens. 4 (2019) 1442–1451, https://doi.org/10.1021/acssensors.9b00680.
[24] P.W. Anderson, Localized orbitals for molecular quantum theory. I. The Hückel Theory, Phys. Rev. 181 (1969) 25, https://doi.org/10.1103/PhysRev.181.25.
[25] R. Hoffmann, An Extended Hückel Theory. I. Hydrocarbons, J. Chem. Phys. 39 (1963) 1397–1412, https://doi.org/10.1063/1.1734456.
[26] R. Hoffmann, Extended Hückel Theory. III. Compounds of Boron and Nitrogen, J. Chem. Phys. 40 (1964) 2474–2480, https://doi.org/10.1063/1.1725550.
[27] P. Bamfield, Chromic Phenomena: The Technological Applications of Colour Chemistry, RSC Cambridge, 2001.
[28] H. Dürr, H.B. Laurent, Photochromism: Molecules and Systems, Elsevier Science, Amsterdam, 2003.
[29] C. Reichardt, Solvatochromic dyes as solvent polarity indicators, Chem. Rev. 94 (1994) 2319–2358, https://doi.org/10.1021/cr00032a005.
[30] J.H. Day, Thermochromism, Chem. Rev. 63 (1963) 65–80, https://doi.org/10.1021/cr60221a005.
[31] M. Mukhopadhyay, S.G. Subramanian, K.V. Durga, D. Sarkar, S. Dasgupta, Laser printing based colorimetric paper sensors for glucose and ketone detection: design, fabrication, and theoretical analysis, Sens. Actuat. B 371 (2022) 132599, https://doi.org/10.1016/j.snb.2022.132599.

[32] S.K. Shannon, G. Barany, Colorimetric Monitoring of Solid-phase Aldehydes using 2, 4-dinitrophenylhydrazine, J. Comb. Chem. 6 (2004) 165–170, https://doi.org/10.1021/cc034033x.
[33] T. Liu, L. Yang, J. Zhang, K. Liu, L. Ding, H. Peng, K.D. Belfield, Y. Fang, Squaraine-hydrazine adducts for fast and colorimetric detection of aldehydes in aqueous media, Sens. Actuat. B 292 (2019) 88–93, https://doi.org/10.1016/j.snb.2019.04.138.
[34] X. Cao, Y. Li, Q. Han, A. Gao, B. Wang, X. Chang, J. Hou, Design of large π-conjugated α-cyanostilbene derivatives as colorimetric sensors for volatile acids and organic amine gases, J. Mater. Chem. C 8 (2020) 4058–4064, https://doi.org/10.1039/C9TC06148g.
[35] L. Sun, A. Rotaru, K. Robeyns, Y. Garcia, A colorimetric sensor for the highly selective, ultra-sensitive, and rapid detection of volatile organic compounds and hazardous gases, Ind. Eng. Chem. Res. 60 (2021) 8788–8798, https://doi.org/10.1021/acs.iecr.1c01389.
[36] R.M. Christie, Colour Chemistry, RSC Cambridge, 2001.
[37] H. Zollinger, Colour Chemistry: Synthesis, Properties, and Applications of Organic Dyes and Pigments, Wiley, Zürich, 2003.
[38] J.R. Askim, M. Mahmoudi, K.S. Suslick, Themed issue: chemical and biological detection, Chem. Soc. Rev. 42 (2013) 8649–8682, https://doi.org/10.1039/c3cs60179j.
[39] Z. Li, J.R. Askim, K.S. Suslick, The optoelectronic nose: colorimetric and fluorometric sensor arrays, Chem. Rev. 119 (2018) 231–292, https://doi.org/10.1021/acs.chemrev.8b00226.
[40] J.R. Askim, K.S. Suslick, Hand-held reader for colorimetric sensor arrays, Anal. Chem. 87 (2015) 7810–7816, https://doi.org/10.1021/acs.analchem.5b01499.
[41] Z. Li, M. Fang, M.K. LaGasse, J.R. Askim, K.S. Suslick, Colorimetric Recognition of Aldehydes and Ketones, Angew. Chem. Int. Ed. 56 (2017) 9860–9863, https://doi.org/10.1002/anie.201705264.
[42] Y. Wang, X. Zhong, D. Huo, Y. Zhao, X. Geng, H. Fa, X. Luo, M. Yang, C. Hou, Fast recognition of trace volatile compounds with a nanoporous dyes-based colorimetric sensor array, Talanta 192 (2019) 407–417, https://doi.org/10.1016/j.talanta.2018.09.028.
[43] N.A. Rakow, A. Sen, M.C. Janzen, J.B. Ponder, K.S. Suslick, Molecular recognition and discrimination of amines with a colorimetric array, Angew. Chem. Int. Ed. 44 (2005) 4528–4532, https://doi.org/10.1002/anie.200500939.
[44] J. Li, C. Hou, D. Huo, M. Yang, H.B. Fa, P. Yang, Development of a colorimetric sensor array for the discrimination of aldehydes, Sens. Actuat. B 196 (2014) 10–17, https://doi.org/10.1016/j.snb.2014.01.054.
[45] J.D. Meyer, M.C. Manning, Hydrophobic ion pairing: altering the solubility properties of biomolecules, Pharm. Res. 15 (1998) 188–193, https://doi.org/10.1023/a:1011998014474.
[46] K.D. Ristroph, R.K. Prud'homme, Hydrophobic ion pairing: encapsulating small molecules peptides, and proteins into nanocarriers, Nanoscale Adv. 1 (2019) 4207–4237, https://doi.org/10.1039/c9na00308h.
[47] J. Schanda, Colorimetry: Understanding the CIE System, John Wiley & Sons, New Jersey, 2007.
[48] S.R. Desai, R.B. Bhoraniya, M. Koladiya, V.V. Bhopekar, C.R. Patel, T. Mori, S. G. Modha, Solvatochromism and halochromism in nitro lophine derivatives: Photophysical study, computational calculations and applications as pH sensing material, J. Photochem. Photobiol. A Chem. 455 (2024) 115751, https://doi.org/10.1016/j.jphotochem.2024.115751.
[49] A.S. Choudhari, S.R. Patil, N. Sekar, Solvatochromism, halochromism, and azo–hydrazone tautomerism in novel V-shaped azo-azine colorants–consolidated experimental and computational approach, Color. Technol. 132 (2016) 387–398, https://doi.org/10.1111/cote.12226.
[50] K.R. Al-Jorani, R.F. Abbas, A.A. Waheb, Synthesis and characterization of a novel benzimidazole derivative: Solvatochromic and acid-base indicator applications, Mater. Today Proc. 42 (2021) 1791–1799.
[51] W.L. Semon, V.R. Damerell, A simplified method for the preparation of dimethylglyoxime, J. Am. Chem. Soc. 47 (1925) 2033–2039, https://doi.org/10.1021/ja01684a037.
[52] W.L. Semon, V.R. Damerell, Sodium hydroxylamine sulfonate as a reagent for the preparation of oximes, J. Am. Chem. Soc. 46 (1924) 1290–1293, https://doi.org/10.1021/ja01670a023.
[53] C.K. Ingold, Principles of an electronic theory of organic reactions, Chem. Rev. 15 (1934) 225–274, https://doi.org/10.1021/cr60051a003.
[54] K. Plataniotis, A.N. Venetsanopoulos, Color Image Processing and Applications, Springer Science & Business Media, Berlin, 2000.
[55] E. A. Feisner, R. Reed, (2013). Color Studies, Fairchild Books, New York, 2013.
[56] D.L. Pavia, G.M. Lampman, G.S. Kriz, J.A. Vyvyan, Introduction to Spectroscopy, Cengage Learning, Massachusetts, 2008.
[57] J. Janata, Principles of Chemical Sensors, Springer Science & Business Media, New York, 2010.
[58] E. Schoolaert, R. Hoogenboom, K.D. Clerck, Colorimetric nanofibers as optical sensors, Adv. Funct. Mater. 27 (2017) 1702646, https://doi.org/10.1002/adfm.201702646.
[59] X. Wang, Y. Si, J. Wang, B. Ding, J. Yu, S.S. Al-Deyab, A facile and highly sensitive colorimetric sensor for the detection of formaldehyde based on electro-spinning/netting nano-fiber/nets, Sens. Actuat. B 163 (2012) 186–193, https://doi.org/10.1016/j.snb.2012.01.033.
[60] J. Wilson, R. Lowery, The Ketogenic Bible, Victory Belt Publishing, Nevada, 2017.
[61] J.C. Anderson, Measuring breath acetone for monitoring fat loss, Obesity 23 (2015) 2327–2334.